Scratch tests to contribute designing performance maps of multilayer polymeric coatings ☆

Yann Rudermann [a], Alain Iost [a], Maxence Bigerelle [b,*]

[a] Arts et Metiers ParisTech, LML, CNRS UMR 8107, 8 Boulevard Louis XIV, 59000 Lille, France
[b] Laboratoire Roberval, CNRS UMR 6253, UTC Centre de Royallieu, BP 20529 Compiègne, France

A B S T R A C T

The scratching technique has gained interest in recent times because of the numerous inherent properties implied (adherence, hardness, elasticity, visco-elasticity, cohesion, etc.) during tests. Some singular mechanical responses have been noticed (cyclical slips and unsticking, degradation modes, etc.) and valued on multilayers polymeric coatings. The results allow differentiating them and illustrating the mare resistance for part. Scratch test is identified as one of the most efficient to build coating performance maps. The main purpose of our work related to the characterization of multilayers polymeric coatings, is to determine a set of experiments in order to compare their mar resistance. Experiments are made by indentation (hardness, creep, stress relaxation), scratch test (determination of the critical load), glossy reflection and wear. In this paper we describe the scratch experiments used to compare the mar resistance of the coatings. The parameters recorded are used to build a performance map relative to a specimen and this performance map is used to compare all characteristics of different multilayers coatings. Two organic systems are taken as samples to illustrate it. They are composed of three layers with a common steel sheet substrate and a common PET topcoat. The intermediary layer is soft and thick for the first product while it is hard and thin for the second one. The scratch results combined with other test results in performances maps underline the role of an intermediary layer in order finally to better design multilayer polymeric coatings.

Keywords:
Polymeric coating
Scratch test
Performance maps
Mar resistance

1. Introduction

The pre-painted steel sheets are complex systems made of several layers whom global properties are difficult to evaluate. The mar resistance is the combination of the individual mechanical properties of the different components (metallic and organic), viewed as the global behaviour of the product in its final environment and the related constraints. Designers need to qualify this resistance, and more precisely to highlight the interactions and the combinations of individual properties. The approach is presently only chemical, driving to well predict the durability of the system but not to investigate the mechanical strengths and leaks of every composition. While using a large range of tests (hardness, abrasion, scratch, etc.), it becomes possible to identify specific fields of performances and build maps to have a global view of the product mare resistance and be certain of the associated market segment (automobile, industrial, electrical appliances, etc.).

The scratch is one of the more efficient tools to reach this goal. This paper deals first with the generation mechanisms and morphology of scratches realised on two different industrial products. Both of them are composed of three layers (Fig. 1). The substrate is a hot galvanized Z100 steel sheet (100 g/mm^2); the intermediate layer is a 120 μm PP soft material (Polypropylene) colaminated to the primary layer for the sample A and a pulverised harder layer of 20 μm (primary gloss paint) for the sample B. The topcoat is a Polyethylene Terephthlate layer (PET) glued in case A and heat-colaminated in case B.

Previous works based on hardness properties [1] have pointed at the large range of mechanical properties such as elasticity, visco-elasticity, plasticity, adherence of layers, etc., but have not allowed assessing the global behaviour of systems under stress [2,3]. Scratch tests are suitable for characterising materials having strong time-and-strain dependent properties [4]. This technique mainly based on friction evolution registration is combined with optical, scanning electron microscopy, and contact profilometry to compare scratches and identify the intermediate layer contribution to the global mar resistance of our samples. Their final performance maps are presented at last to underline the deep contribution of scratch testes to build performance maps and differentiate products (Table 1).

☆ This paper was presented at the 36th Leeds–Lyon Symposium on Tribology, Lyon 2009.

* Corresponding author.
E-mail address: maxence.bigerelle@utc.fr.(M. Bigerelle)

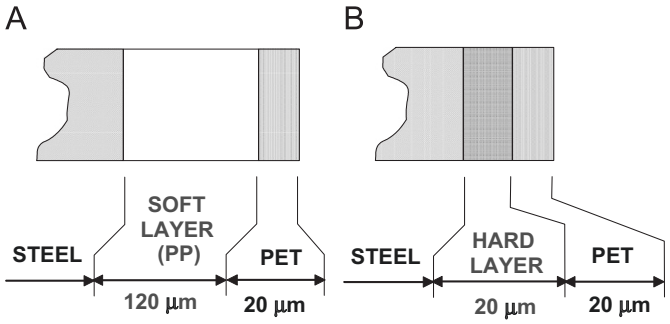

Fig. 1. Constitution of products A and B.

Table 1
Symbol meaning.

Symbol	Explanation
A	Scratched Area (μm^2)
a_1	First half scratch width (μm)
a_2	Second half scratch width (μm)
B	Pads areas (μm^2)
Fn	Applied load (N)
h_i	Elastic return (μm)
h_b	Pads height (μm)
L	Width between pads (μm)
LC	Critical load
P	Indentation depth (μm)

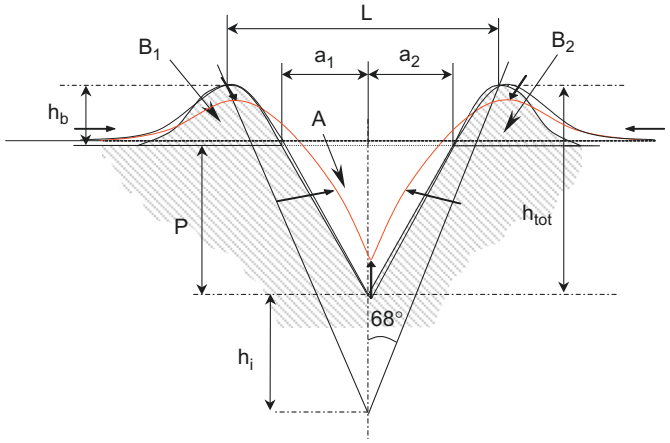

Fig. 2. Characteristic areas and length of a scratch track. Model of evolution of a scratch track between the moment indenter scratches system and the end of visco-elasticity come back (see Table 1 for symbol explanation).

2. Experimental

2.1. Samples and hypothesis

Pre-painted steel sheets are systems whose homogeneity is granted by mechanical, electrical, thermo dynamical or/and chemical forces. Adhesion is then viewed as a volume property because of strength gradients created between layers [5]. The scratch test puts into trial numerous adhesion phenomenons depending on the force put on the indenter. It is the reason why Consiglio et al. [6] considered it as one of the most efficient method to quantify the adhesion properties of polymer films. Preliminary works (MEB analysis of the layers, the inter-phases and the interfaces edgewise) have driven to observe that the chemical interface sub-layer/PET is nearly the same whatever is the system; the topcoat adhesion is then considered to have minor influence on the overall conclusions and observations.

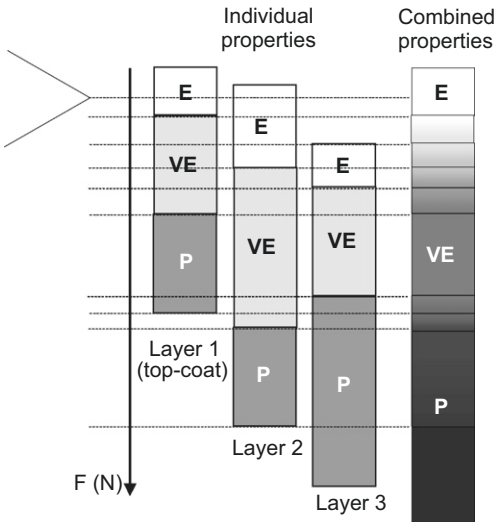

Fig. 3. Projection of the resulting mechanical properties on a product composed of several layers with variable properties according to their thickness and the nature of the combinations. Remark: according to the thickness and the properties of the materials some systems could present sequences of singular distortion modes (e.g. E-elasticity, VE-visco-elasticity, P-plasticity).

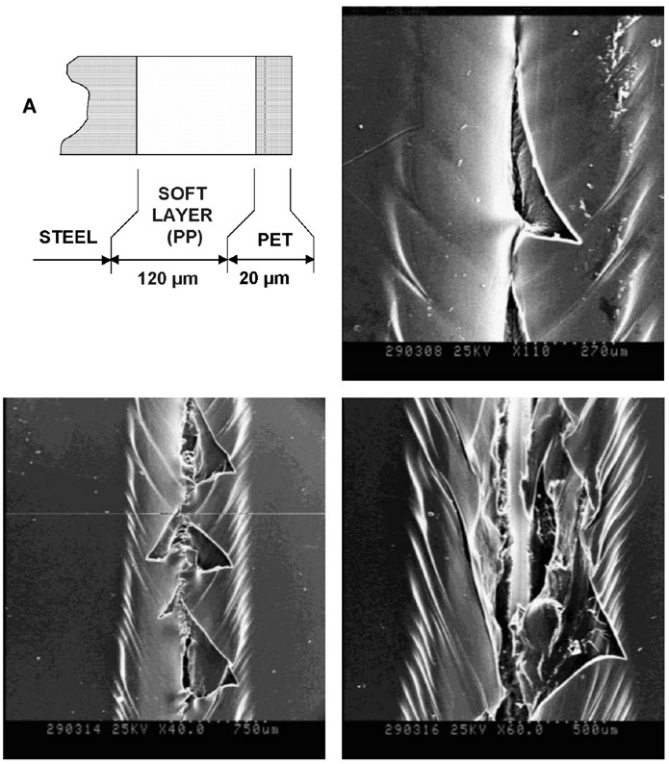

Fig. 4. Constitution and morphologies of scratch on product A; every photo illustrates a different deformation mode—mode I (on top and right: low amplitude ruptures), mode II (on bottom and left: shortcoming increase to critical size) and mode III (on bottom and right: delaminating and remnants).

Scratch test being a contact-based experiment in a dynamical process, the surface analysis of the samples has insured that their roughness (Ra = 11 μm in both cases) do not influence the results.

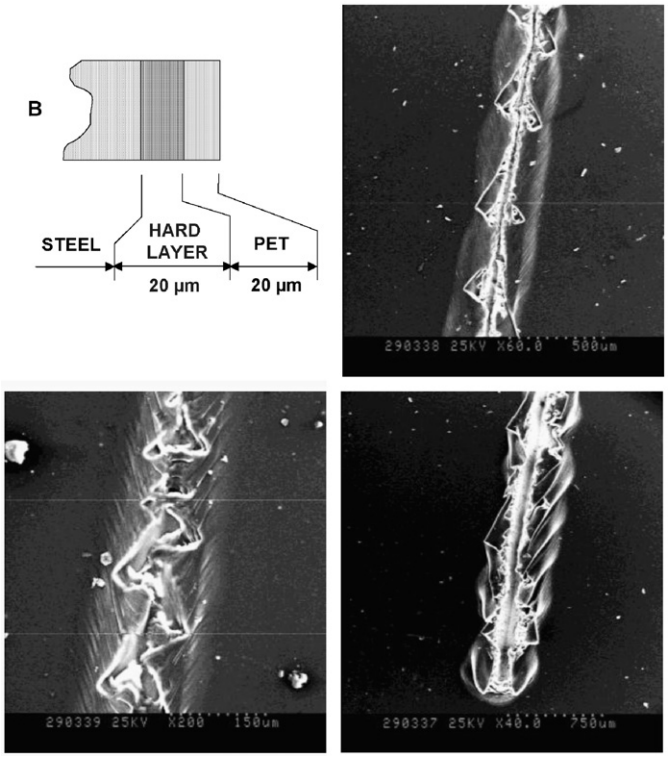

Fig. 5. Constitution and morphologies of scratch on product B; every photo illustrates a different deformation mode—mode I (on top and right: low amplitude ruptures), mode II (on bottom and left: shortcoming increase to critical size) and mode III (on bottom and right: delaminating and remnants).

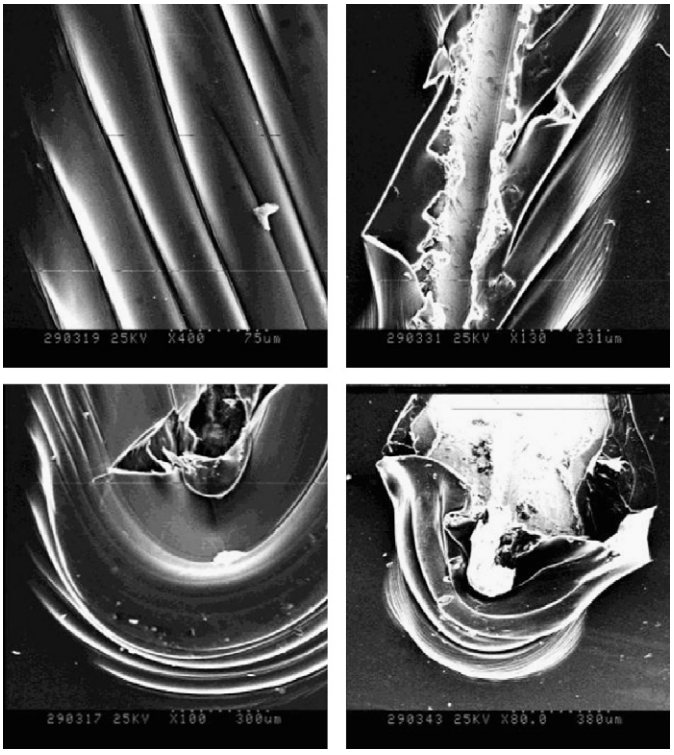

Fig. 6. Notification of the periodical formation of "draped of matter" along and at the end of the track.

2.2. Method

2.2.1. Scratching and friction coefficient

The load range is (0–30 N) and varies with according to V_F–law expressed in N/min. The samples are attached on a moving table allowing a constant scratch velocity V_l from 0.01 to 60 mm/min. The evaluation length of scratch L equals 15 mm. Even though systems are sensitive to scratching velocities [7] V_l has been fixed to 15 mm/min (optimal noticed velocity).

Three tests are realised on each sample in order to identify with certainty the critical loads. They are loads for which the friction coefficient signal changes suddenly of slope and/or mean value.

Table 2
Average critical loads measured for a constant advance speed of 15.92 mm/min.

Loading rate (N/min)	Critical loads (N)		
	LC1	*LC2*	*LC3*
Sample A			
12	7.0	–	–
20	7.5	13.6	–
30	6.5	13.0	–
40	7.4	14.1	–
50	8.1	13.9	–
Sample B			
14	1.5	5.0	9.8
20	1.7	6.3	10.8
25	1.7	5.8	9.8
35	2.0	5.8	10.5

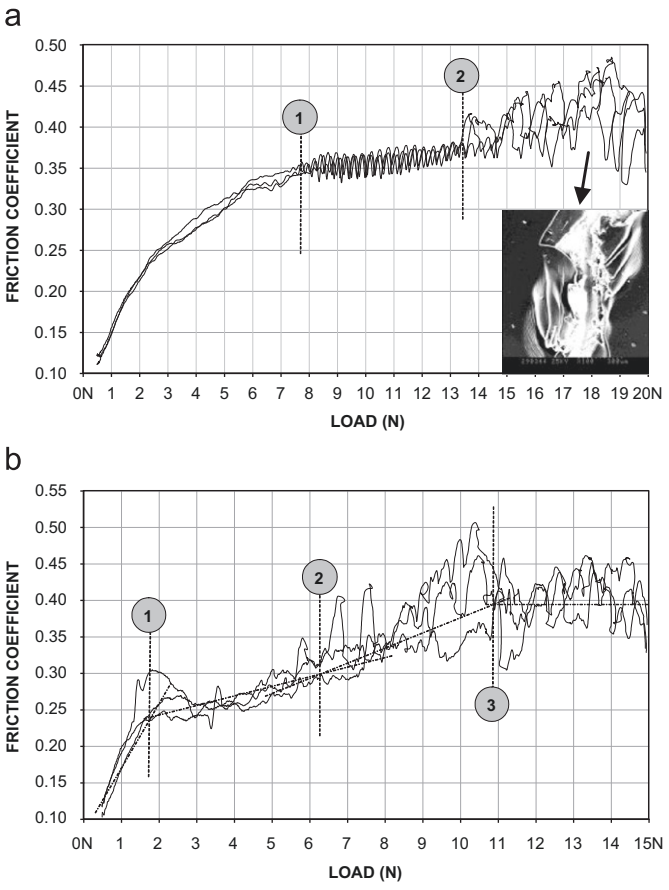

Fig. 7. Record of the friction coefficient for product A (a) and product B (b) according to the load with a graphical determination of the two first critical loads (see Table 2).

The Vickers indenter has a large tip radius of 200 μm in order to have a better distribution of contact pressures (Hertz constraints) on the frontal pad and to better observe the elastic properties [8]. The indenter holder is connected to piezoelectric transducers to record the actual normal load (slightly different of the consign) and the related tangent loads.

2.2.2. Surface profilometry and SEM studies

Scratches are rebuilt numerically with a three dimensional (3D) tactile roughness profilometer KLA TENCOR P10 to appreciate their topological evolution with the load and to design the corresponding model (Fig. 2). This latter device consists of a diamond tip with a 2 μm rounded-end having a 10 nm vertical resolution according to the manufacturer.

The successive distortion modes (cyclic formation, progressive cracks) are identified while correlating pictures taken with scanning electronic microscopy (SEM) and the friction diagram.

2.3. Data analysis

Whatever is the considered product, the mechanical properties are always implied in the same order [9], depending on the implied strain: elasticity (weak loads with a quasi total recover of the print), visco-elasticity (observed after discharge and enough time to observe "the skinning") and visco-plasticity (out-flow around the indenter and lateral pads).

The model underlines well that due to visco-elasticity properties, the track sides are actually curved. As a consequence h_i and L lengths are not reliable data; searching for optimal tangent lines

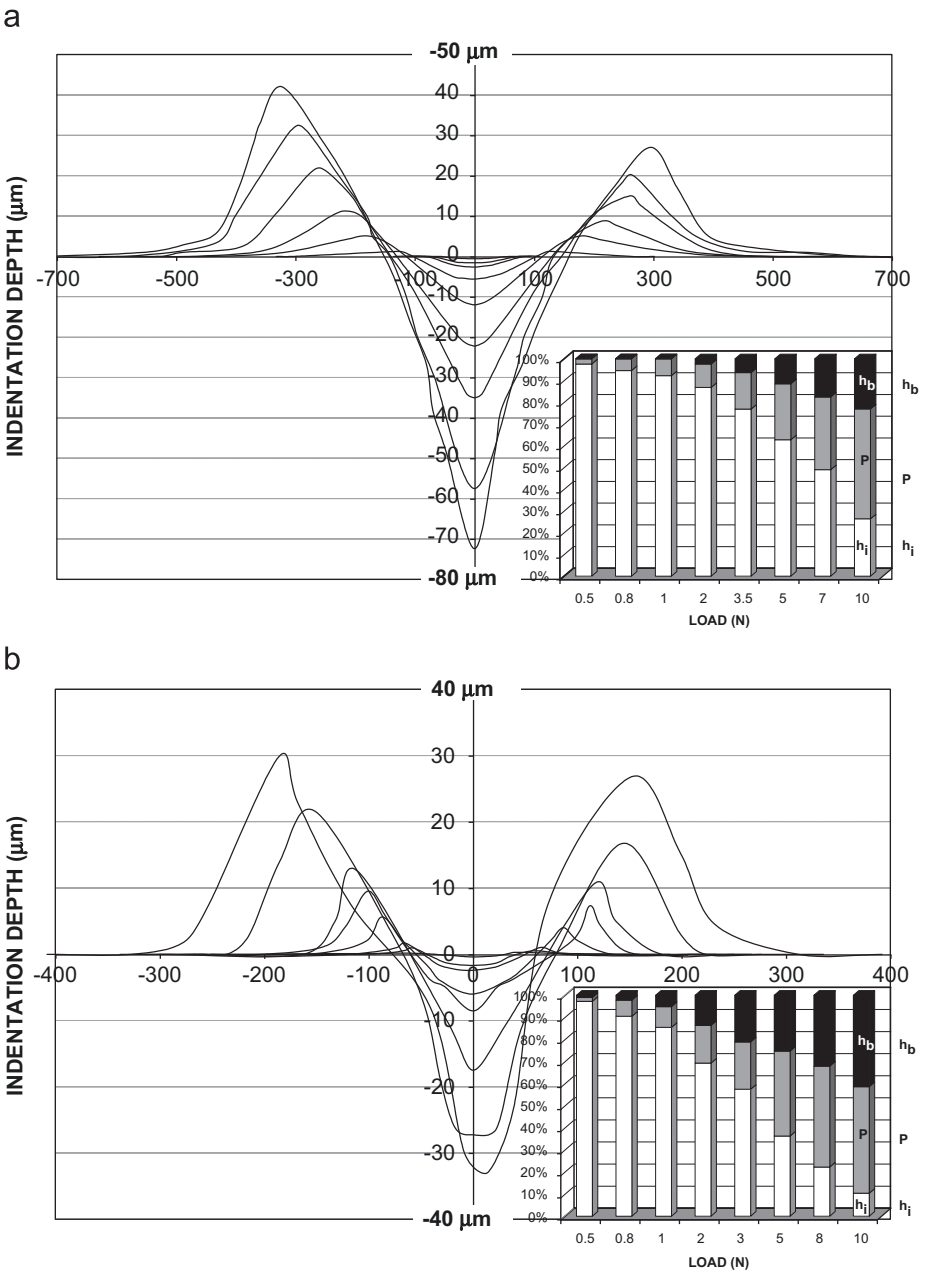

Fig. 8. 2D scratch profile evolution for loads comprised between 0.5 and 12 N. Bar chart of the distortion proportions for each applied load (h_i for elasticity, P for plasticity and h_b for visco-elasto-plasticity) for product A (a) and product B (b).

being a complex work, the analysis is achieved while considering straight lines (Fig. 2). The following relations define then the relative proportions of distortions:

$$X_e = \frac{h_i}{h_i + h_b + P} \tag{1}$$

$$X_{vp} = \frac{h_b}{h_i + h_b + P} \tag{2}$$

$$X_P = \frac{P}{h_i + h_b + P} \tag{3}$$

The scratch hardness, valued by analogy with indentation tests, is also assessed

$$H_s = q\frac{4F}{\pi a^2} \tag{4}$$

where F is the normal load applied on the indenter, a is the scratch width (Fig. 2, $a = a_1 + a_2$) and q is a material-based parameter. The measured hardness of multilayer systems is a combination of the different layer properties, varying with the indentation depth (Fig. 3). In this case q is a complex function depending of F, varying deeply every time the indenter-led strains reach a new layer.

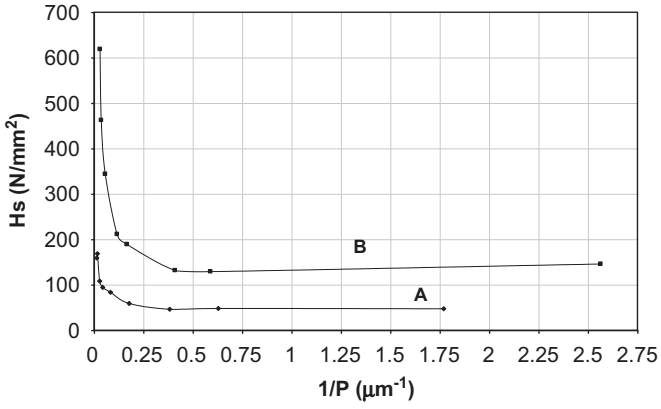

Fig. 9. Relationship between hardness H_s and the inverse of the penetrating length $1/P$.

3. Result and discussion

3.1. Morphology analysis

Studied products, having a same PET topcoat, have comparable morphologies as Figs. 4 and 5 underline it.

Descriptions of scratches have already been realised by Briscoe et al. [4] to characterise bulk polymeric materials; for scratches realised on multilayered systems it deals as follow.

For low loads, the distortions have no large amplitudes, they are not visible to eye. The distortions of mode I, marked by PET cracks in bones along the track axis and the formation of "drapes of matter", appear owing to local adherence losses.

The mode II follows with a larger opening of the topcoat and the amplification of drapes (Fig. 6) with a 45 µm-period, explained by the visco-elasticity properties of the PET (semi-crystalline) known for its capacity to undertake a partial reorganization of its micro-structure when it is submitted to surface constraints.

The influence of a repetitive slip effect in front of the indenter reaching regularly the PET elastic limit is also noticeable.

Finally, the deformations of mode III correspond to a critical stage when the matter extortions and the scoring of the galvanized steel sheet begin. Whereas product *A* has more and more ruptures with periodic drapes and weak detachments, the product *B* has reached an ultimate stage with the complete take-off of the topcoat.

3.2. Friction

Modes II and III underline the creation of remnants and the passage of the indenter through the organic layers. It appears with an increase of the friction due to the development of the indenter/material contact area and to the passage from a polymeric friction to a metallic one.

Inside a same distortion domain, the friction coefficient increases linearly, oscillating around a mean value. At the passage of one distortion mode to the next one, the oscillations are amplified because the system distorts itself more and more: rough surfaces are created and the contact areas increase considerably. The modification of the slope of the mean-value lines allows identifying the critical loads (Table 2, Fig. 7).

- *LC1*: mode 0/I; mode 0 is the initiation of the scratch (neither material detachment nor cracks) with little plastic distortions and the creation of lateral pads.

Table 3
Results for the scratch parameters (see Fig. 2 for the definition of sizes).

Fn applied load (N)	*P* indentation depth (µm)	h_i elastic return (µm)	h_b pads height (µm)	*A* scratched area (µm²)	*B* pads areas (µm²)	*L* width between pads (µm)	a_1 half scratch width (µm)	a_2 half scratch width (µm)
Sample A								
0.5	0.57	22.91	0.00	0	0	116	−58.0	58.0
0.8	1.59	27.96	0.00	0	0	146	−73.0	73.0
1.0	2.61	30.98	0.00	0	0	166	−83.0	83.0
2.0	5.63	45.33	1.25	717	232	258	−104.0	104.0
3.5	12.00	54.73	4.50	1550	1374	352	−115.0	116.0
5.0	22.50	54.72	10.00	3177	2760	431	−130.0	130.0
7.0	35.00	51.22	18.40	5002	5428	517	−140.0	147.0
10.0	57.50	29.98	26.25	7947	8552	562	−142.0	133.0
12.0	72.40	18.36	34.50	9778	11,154	619	−150.0	160.0
Sample B								
0.5	0.39	21.65	0.22	16	30	110	−35.0	31.1
0.8	1.70	21.06	0.52	97	36	115	−44.5	44.4
1.0	2.44	22.14	1.32	197	63	128	−47.8	50.6
2.0	6.00	24.40	4.81	423	324	174	−54.6	61.5
3.0	8.54	22.91	8.41	569	663	197	−59.0	75.5
5.0	17.50	16.53	11.50	1197	1063	225	−62.4	73.7
8.8	27.25	13.29	19.15	2304	2926	295	−68.5	80.0
10.0	33.00	7.10	28.30	2466	5692	338	−79.5	64.0

- *LC2*: modes I/II; mode I appears with ruptures of weak amplitude of the topcoat, in bones or droplets, along the main axis of the scratch. The first lateral distortions, without detachment of material, are included in this mode. Mode II corresponds the amplification of the type-I shortcomings, reaching critical sizes. The top layer distorts itself under the constraint (periodic drapes).
- *LC3*: modes II/III; this final mode is characterized by delamination of layers with the creation of remnants and accordion-like withdrawals. The streak is enough deep to reach the galvanized layer. The organic system is ruined and does not protect the metallic substratum anymore.

3.3. *Topography of scratches and mechanical properties of systems*

Analysing the streak along its main axis with a 3D-profilometer, we extracted the successive 2D profiles to observe their geometrical evolution with the load (Fig. 8).

The additional bar charts allow appreciating the mechanical properties entering in the distortion phenomena according to the applied load. The elastic properties are only predominant for low loads and yield quickly place to plastic distortions. To note all the same that the plastic distortion rate is practically equal for the two products at the highest loads, whereas the elastic distortions are even dominant for the product A: this is the whole profit of an intermediate layer with dominant visco-elastic properties having an enough large thickness to distribute contact pressures.

The B-product PP intermediate layer also explains the almost constant hardness difference between the two products at the low loads (Fig. 9, high $1/h_i$). The hardness, measured from the surface appears therefore less important, notably because of the PP visco-elastic properties encouraging the indenter penetration while protecting the system more efficiently (Table 3).

4. Multilayer organic coatings performance maps

The results issued from scratch tests are integrated to performances maps with a panel of other characteristically values. They are distributed into five main categories:

- Durability and product morphology (roughness, accelerated ageing tests, damage velocity, etc.)
- Deformation energies
- Hardness related parameters
- Scratch tests critical loads
- Perception related parameters (reflection, gloss, etc.)

The point here is to underline the deep contribution of the scratch tests in the global evaluation of performances of multilayer coatings. Fig. 10a and b shows the maps realised, respectively, for products A and B. As a comparison, a third product (D), 25 μm-thick composed of only two thin layers is presented (Fig. 10c).

The maps underline the specific contribution of the intermediate layer of product A: good performances in deformation energies and damage classes. The high elasticity and visco-elasticity properties of the PP allow absorbing deformation energy and mask damage. On the contrary, under high abrasive solicitation (durability/morphology class), the product A has very poor performance. The intermediate layer also implies higher critical loads under scratch, even if finally the scratches are easier to identify (low performance in perception class due to large and deep prints). Product A appears better than B, but not at all, it depends on the ratio efficiency/actual and final solicitations. The performance maps drive to categorize the multilayer products and their ability to integrate or not a given market.

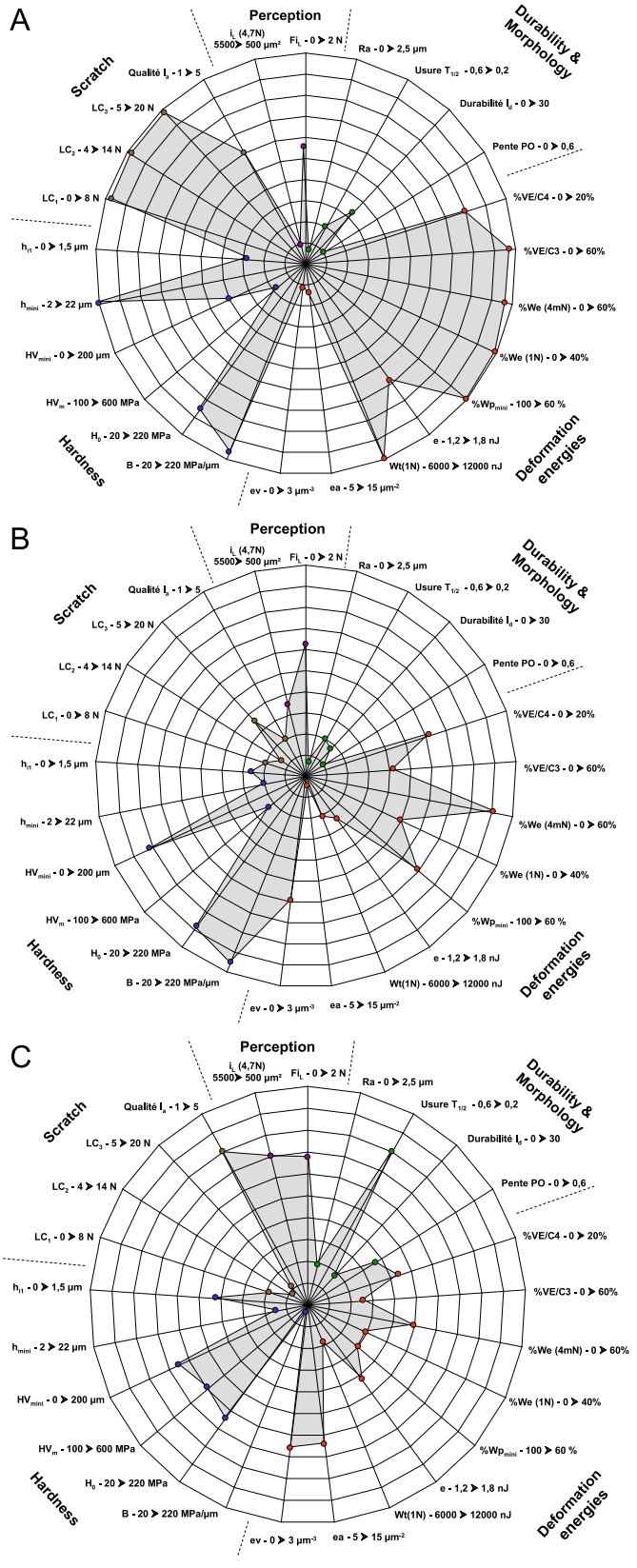

Fig. 10. Performance maps of products A, B and C.

5. Conclusion

The experiments carried out on two three-layer products have highlighted the predominant role of the intermediary layer material (the substrata and the topcoats being the same) on their global mare resistance. If we cannot pull quantitative information characterizing directly this resistance, it does not remain less than scratch tests associated to MEB observations, 3D and 2D surface profilometry and friction evolution records are well designed to appreciate the ability of new products to undergo surface stresses. Particularly it has been possible to show the great interest to intercalate an enough thick soft layer between a steel sheet and its PET topcoat. Applying again this method it would be possible to define the best material to use and to calculate the related best layer thickness to improve the system global performances (maps) and mar resistance.

Acknowledgement

Authors want to thank Stéphane Benayoun, LTDS Lyon, for his help in scratch-test experimentation and for fruitful discussions.

References

[1] Iost A, Najjar D, Hellouin R. Modelling of the Vickers hardness of paint coatings deposited on metallic substrates. Surf. Coat. Technol. 2003;165:126–132.

[2] Pelletier H, Duriera AL, Gauthier A, Schirrer R. Viscoelastic and elastic–plastic behaviors of amorphous polymeric surfaces during scratch. Tribol. Int. 2008;41: 975–984.

[3] Jardret V, Zahouani H, Loubet JL, Mathia TG. Understanding and quantification of elastic and plastic deformation during a scratch test. Wear 1998;218: 8–14.

[4] Briscoe BJ, Evans PD, Pellilo E, Sinha SK. Scratching maps for polymers. Wear 1996;200:137–147.

[5] Champetier G, Rabaté H. Physique des peintures, vernis et pigments, tomes 1 et 2. Paris: Dunod; 1962.

[6] Consiglio R, Randall NX, Bellaton B, Von Stebut J. The nano-scratch tester (NST) as a new tool for assessing the strength of ultrathin hard coatings and the mar resistance of polymer films. Thin Solid Films 1998;332:151–156.

[7] Randall NX, Favaro G, Frankel CH. The effect of intrinsic parameters on the critical load as measured with the scratch test method. Surf. Coat. Technol. 2001;137:146–151.

[8] Lange J. Development of scratch tests for pre-painted metal sheet and the influence of paint properties on the scratch resistance. J. Mater. Process. Technol. 1998;86:300–305.

[9] Low IM. Effects of load and time on the hardness of a viscoelastic polymer. Mater. Res. Bull. 1998;33:1753–1758.